March 1985

TAE No. 509

DURABILITY UNDER REPEATED BUCKLING OF

STIFFENED SHEAR PANELS

by

M. Kollet

T. Weller

A. Libai

J. Singer

Scientific Report No. 5

AD-A167 596

86 5 1 029

March 1983

DURABILITY UNDER REPEATED BUCKLING OF
STIFFENED SHEAR PANELS

by

M. Kollet

T. Weller

A. Libai

J. Singer

Department of Aeronautical Engineering

Technion - Israel Institute of Technology

Haifa, Israel

TABLE OF CONTENTS

ABSTRACT

An experimental investigation was carried out on the durability of thin webbed beams subjected to repeated shear bucklings. Although the repeated loading exceeded the initial buckling load several times, it was in the range of 25% to 50% of the ultimate loads, which is well within the flight evelope of many airframes. Initiation and propagation of fatigue cracks up to complete failure was followed during the tests. An empirical life prediction formula based on this test series was developed and will be updated by further testing.

The experimental investigation was supplemented by numerical analysis using the STAGS computer program.

The number of load cycles to crack initiation, N_i, and the fatigue failure N_f, ranged in this test series from about 20,000 cycles to about 200,000 cycles.

It appears that the most significant parameter affecting N_f was the ratio of ultimate to cycling loads.

NOTATION

A	correlation parameter
a_0	amplitude of assumed imperfection
b	distance between uprights (ss Fig. 2)
d	overall height of Wagner beam (see Fig. 2)
I_f, I_u	area moment of inertia of flange and upright cross sections respectively
J_f, J_u	torsional moment of inertia of flange and upright cross sections respectively
N_i	number of cycles to crack initiation
N_f	number of cycles to failure in fatigue
t	web thickness
V	external shear force
$(V_{cr})_{exp}$	experimental external shear force at buckling
$(V_{cr})_{cal}$	calculated external shear force at buckling
$(V_{ult})_{exp}$	experimental external shear force at ultimate failure
$(V_{ult})_{cal}$	calculated external shear force at ultimate failure
V_y	external shear force at which local yielding first occurs
w	transverse deflection of beam
w_0	initial imperfection
α, β, γ	correlation parameters

LIST OF TABLES

LIST OF FIGURES

1. INTRODUCTION

Stiffened plates and panels can withstand shear loads far in excess
of their initial buckling loads before they fail. This stable postbuck-
ling behavior has been an important factor in many aeronautical engineering
designs, especially where strength is the primary design criteria and redu-
ction of structural weight is at a premium. The structural model which
is commonly used for the analysis of this phenomenon is the theory of
"diagonal tension", first introduced by Wagner [2] for the case of rigid
stiffeners. It was further developed by Kuhn and his associates to include
the effects of the tension field on the compressive load carrying capabi-
lity of the plate. Also included were the effects of the in-plane flexibi-
lity of the stiffeners and the participation of the plate in the loads car-
ried by the stiffeners. This resulted in the theory of "incomplete diago-
nal tension" which is summarized in [3-6].

During the fifties and sixties, utilization of the stable postbuckling
behavior of plates in shear was extended to civil engineering applications,
mainly for plate girder design. Some results of these studies are summari-
zed in [1], where an extensive list of references is also supplied. In most
civil engineering designs the flanges of the plate girder are relatively
flexible and the mode of ultimate failure can be flange collapse rather than
web tear. Also, the depth of the wave pattern in the web is affected by the
flange flexibility. The criterion introduced by Rockey[7] can be used to
estimate the importance of this effect. See also equation (1) of [1].

The designs based on criteria developed by tension field theory and by the civil engineering criteria of flange failure, considered the static ultimate load carrying capability of the web-stiffener system in shear as the prime factor to be taken into account. Therefore, all the analyses were aimed at the determination of the ultimate shear load, V_{ult}. Details of the stress distribution at the working loads were not supplied and were not considered to be worth the effort of obtaining them, provided that the ultimate margin of safety was adequate. In any case, these details were difficult to calculate and even now, with the extensive capability of computational facilities, "a full-fledged nonlinear analysis that utilizes the necessary refined grid to model the actual structure is prohibitively expensive and therefore unrealistic from a computational and design point of view[8]."

Two additional factors have been added during recent years which have led to the need for reappraisal of the subject. The first is the appearance of new materials for the design of primary parts of aircraft. Among these, higher strength metals and composites are the more noteworthy. The second (and of no lesser importance) factor is the steady increase in the number and relative levels of repeated load applications during the expected lifetime of the aircraft, as a result of more optimal designs and of better utilization and extended life of airplane fleets.

The main concern is that parts which are designed to be subjected to many repeated bucklings during their lifetimes may fail prematurely in fatigue. The danger increases with the number of bucklings, the level of the shearing loads above the initial buckling load, and the susceptibility of the material to local effects caused by the high localized bending stresses

which are superimposed on the in-plane stresses. The problem also came up in civil engineering applications [9-11].

This concern, supplemented by recent service failures which could be attributed to repeated bucklings, provided the general motivation for the present study. The results reported here are confined to metal beams, and the material utilized is Aluminum 2024T3, which is one of the standard materials in aircraft manufacturing. Extension to composite beams will be made at a later stage.

Direct literature on the durability and fatigue failures of stiffened shear panels subjected to repeated bucklings, is not extensive. Reference [12] discusses NASTRAN calculations and accompanying tests on a series of integrally stiffened Wagner beams. The results of the numerical calculations (stresses at the crests of the waves) were utilized in order to obtain equivalent notch stresses. The latter formed the basis of a fatigue analysis which was correlated with the experiments. Correlation factors were introduced as necessary. The main emphasis in the series was on a range of ultimate-shear/buckling - shear ratios of 2-3 (which is lower than the range to be represented in this report).

Reference [13] presents a series of fatigue tests on stiffened composite shear panels. Both web cracking due to severe bending and stiffened web separations were noted. A supporting analysis using NASTRAN was also performed. Interaction of the buckled waves with the surrounding structure were not taken into account in the analysis. Additional tests on buckled composite shear panels are reported in [14, 15, 16, 19].

The initiation of fatigue cracks at the points of the most severe bending in buckled shear panels was noted in Reference [17] . The tests were conducted on aluminum panels and the results agreed reasonably well with estimates based on SN diagrams.

Analytical and numerical calculations of the postbuckling behavior of stiffened shear panels can be useful for the prediction of the crack nucleation stage of the fatigue life. Even so, they are rather limited in scope, since the local modification of the stress fields due to inelastic strains or the severe localized stress concentrations are extremely difficult to obtain.

The analysis can predict the overall behavior including the number, amplitude and inclination of diagonal waves and also the effects of the surrounding structure on the deformation parameters. Energy methods appear to be most useful in this respect [18, 19].

The numerical calculations can use one of several computer codes which have nonlinear capability for plate and shell elements. The programs which were most extensively used were NASTRAN [20] and STAGS [21]. Some of the calculations were used for comparisons with experiments. See for example [8, 13, 17, 22, 23, 24]. It appears from the results of the calculations that overall behavior can be predicted rather accurately but the results of detailed stress distributions are less conclusive.

The effects of the surrounding structure (stiffeners, stress environments) on the durability of repeatedly buckled panels are very important. Not only do the stiffeners influence the overall behavior, but

they also contribute very strongly to the severe local effects near the corners of the panel - where most fatigue cracks initiate. In fact, many of of the fatigue failures in the tests reported above and in other tests, started at the stiffener (or flange) panel boundaries near the corners of the tension diagonal. Thus in order to obtain realistic and meaningful information on the durability of shear panels, they have to be tested in a realistic environment, with realistic stiffeners and flanges, and with the correct transmission of the shearing loads from the neighboring structure.

Based on the above considerations and on preliminary testing [1], a three point loading Wagner beam configuration was decided upon for this test series. The need for mutual interaction between the shear panel and the flexible stiffeners and flanges ruled out the possibility of a "picture frame" testing (the effects of additional moments which are inherent to the three-point loading configuration, although of no major importance, were considered to contribute to the realistic environment).

The stiffeners and flanges of the Wagner beams were bonded to the shear panel according to aeronautical specifications. The fact that there was no bonding fatigue failure during the entire test series is indicative of the integrity of the bonding. It provided a realistic support condition and, on the other hand, it was not a "weak link" in the test system. The success of the bonding in this series of rather severe postbuckling cycling tests is an important result although it was not an initial requirement of this research.

It is recognized that the durability of repeatedly buckled panels in a realistic environment is both a multiparameter problem and one for which

the statistical nature of fatigue behavior should apply. Therefore, any single test series must limit its scope and vary only a few of the parameters. Within the Wagner beam configuration which was chosen to be tested, the following effects were studied and corresponding parameters varied:

a. Effect of the surrounding structure - by varying the size of the stiffness and flanges (three sizes were used).

b. Effects of the magnitude of the initial buckling load - by varying the web thickness (three web thicknesses were used).

c. Effects of the shear loading (compared with the initial buckling shear V_{cr} and the ultimate shear V_{ult}) - by varying the magnitudes of the repeated loads V_{cyc} from test to test. The range of the applied repeated loads was on the high side: several times the initial buckling loads and up to 1/2 V_{ult}. The main considerations for this choice were the need to investigate the effects of severe buckling on one hand and to maintain the loads within range of possible fatigue spectra of existing modern day airplanes on the other hand.

A constant load amplitude of $0 - V_{cyc}$ was maintained within each test. Spectrum testing was ruled out for this series in order to limit the number of test variables. The possibility of doing some spectrum testing in a future series is envigased. Such results could be checked against test-oriented cumulative damage predictions based on the present series.

Material properties were not varied in this test series and all the tests were conducted on 2024T3 aluminum specimens. Extension to composite beams of similar configurations is planned.

Further details of the test specimens, setup and experimental procedures are given in the subsequent sections.

Some of the important test parameters are grouped into nondimensional forms and a correlation study was initiated in order to arrive at a semi-empirical "test formula". This formula should be checked for its predictive capability against the various tests performed as well as against future tests. Apart from its obvious practical potential as a design tool, it can contribute towards the understanding of the relative importance of the various parameters in determining the fatigue behavior. This phase of the research is still under investigation and will be continued throughout the entire test series, including future tests. Progress in this important aspect of the research is reported in a subsequent section.

The STAGS computer program was chosen for numerical support to the research and calculations of the strong postbuckling behavior of the panels and surrounding structure were conducted. After overcoming initial difficulties, good correlation between tests and calculations was obtained by taking the initial imperfections as two trigonometric double sine terms with amplitude equal to the web thickness. Apart from overall support to the testing program, the calculations can be used for specific purposes such as the numerical determination of the load level at which inelastic stresses first occur in the susceptible region near the corner. This load may become an important design parameter in view of the well known influence of local inelastic stresses on low cycle fatigue behavior. Some of the numerical results are presented in this report.

2. TEST SETUP & PROCEDURES.

The test setup is shown in Fig. 1. The load experienced by the beam specimen in the loading frame of this setup is of a three point loading type; the load is introduced through a pin into the center of the beam by a hydraulic jack via a load cell connected to two heavy parallel vertical bars, into which the pin is inserted. The load is controlled through an MTS system that permits precise control of applied load and frequency loading ranges from zero to maximum load (in a const. amp. mode). The edges of the beam are loaded by pins in-serted into the specimen and into two heavy parallel vertical bars at each end, which are simply connected by pins to the loading frame. The reaction loads experienced by these pins are introduced via the uprights into the shear web.

Since allowances for lateral deflections of the specimens may cause premature failure due to lateral instability of the flanges of some of the beam configurations, transverse deflections of the specimens are prevented by means of heavy parallel cross members attached to the loa-ding frame along the top and bottom flanges of the beam. These cross beams permit the restraining of the transverse deflections, only at specified points along the specimen.

The response of the specimens is measured by strain gages bonded to the shear web surfaces, flanges and uprights of the beam specimen and re-corded by a multichannel data logger. Recording of these gages is li-mited to quite a low number of cycles relative to the overall life of the

specimens, because the strain gages cannot sustain the very high cyc-
ling strains experienced by the beams and have a very low endurance
life under such circumstances.

Also, the shadow-moire technique is employed for overall observa-
tion.of the progressive behavior of the buckled shear web, as well as for
comparison of the deflected shape of the beam with predictions by the
STAGS [21], computer code. The grids employed in this technique are
removed when cracks are assumed to initiate, to permit a visual obser-
vation of these cracks and to avoid their being damaged at the failure
of the beam.

Each test was conducted and divided into the following phases:

1. A slow gradual loading of the beam to a load slightly above either
    the predicted or observed shear buckling of the specimen, to deter-
    mine the actual buckling load of the webs of the beam. Then release
    of the load.

2. A slow gradual reloading of the beam to the load of (1) to identify
    any effects of the load in (1) on the critical load observed in (2).
    Then either release of the load, or further increase of the load.

3. In this phase two different procedures of loading were practiced; In
    the first one, gradual loadings of the specimen (WB-6) to determine the
    "permanent buckling" load, was performed. The load was increased
    by specified incraments relative to the preceding load and then re-
    leased. This load was gradually increased in this fashion up to the
    maximum load for repeated loading, the value of which was dictated

by either the strain value at the lower corner of the tension dia-
gonal, or the planned ratio of the repeated working load to the
predicted ultimate load. In some cases the magnitude of the working
load was dictated by both the measured strain at the corner and the
planned loading ratio. It should be noted that the strain value at
the lower corner is usually well in the plastic region and sometimes very
high strains may be observed prior to reaching the planned loading ra-
tio. Therefore, further loading of the specimen can result in very
high strains, which will trigger failure of the beam after a very short
cycling life. Consequently, repeated loading is executed at a smaller
loading ratio than the planned one.

In the second procedure (Beams WB-2 to WB-5 and WB-7 to WB-11), the load
is continuously increases to the maximum load for repeated loading.
The magnitude of this load is determined as in the first procedure.

4. Continuous repeated loading from V=0 to V_{cyc} with interruptions every
few tousand cycles for complete strain gage and moire records. The
beams are loaded at very low frequency (1 to 2.2 Hz).

5. Once a crack initiates and completely penetrates through the thick-
ness of the web, its further growth is continuously measured, moni-
tored and recorded by a video camera and tape till large scale fai-
lure of the web takes place. It should be noted that in order to
avoid complete failure of the whole beam, due to failure of the web,
a stop is introduced in the center of the beam, thus avoiding any
significant damage to the beam at collapse.

6. The beam is removed from the loading frame. The damaged panel is removed and replaced by a stiff dummy one. The beam is then placed back in the loading frame in an inverted position to the repeated loading test. Thus the previously highly stressed and damaged tension field of the web which did not fail, will experience compression stresses and the portion of the web previously loaded in compression will be loaded in tension under further loading of the beam. The beam is now retested statically to failure to determine its ultimate load, which will constitute the actual loading ratio under which the beam was repeatedly loaded. The result is checked against a calculated ultimate load, obtained by a standard diagonal tension analysis [3].

5. TEST SPECIMENS

10 Shear beams were tested. Their dimensions are presented in Fig.2 and Table 1. It can be seen that the test series comprises of beams with three web thicknesses: 0.5 mm, 0.8 mm and 1.0 mm and stiffened by three types of L sections: "light" - L12×12×1.0 mm, "moderate" - L15×15×1.5 mm and "heavy" - L20×20×2 mm. This allows for evaluation of the effects of quite a wide range of stiffening and flexibility of the framing, as reflected by the parameter (I_f/b^3t) and of the corresponding relative magnitude of the buckling, yield and ultimate loads of the beams (see Table 2) on the durability of the beam at the specified cyclic loading condition (see Table 2).

The critical shear and ultimate loads corresponding to the beams given in Table 2, were predicted by Eqs. (32) & (33a) of [3] respectively, as well as by the STAGS computer code [21]. Since this program permits a comprehensive detailed analysis of the beam, it provides information about the "critical" points along and adjacent to the tension diagonal of the web and initiation of yielding there. This information is compared and correlated later with the recorded data by the strain gages adjacent to these "critical" points, to obtain the actual load at initial yielding of the beam.

As can be seen in Fig. 2, the beams consist of five shear webs symmetrically framed by identical L section flanges and uprights. Two of the webs serve as the test section fields. Through the other three, the central one and the edge ones, the three loads are introduced into the beam. These webs are heavily stiffened in a manner which assures almost uniform shear load difusion from the three loading pins into the test panels.

In the early stages of the test program (beams WB-2 to WB-7), the two test sections were tested simultaneously. This was aimed at actually doubling the number of test data points, as well as confirming the almost symmetrical loading behavior of the test rig. However, the actual ultimate load was required for each specimen to determine its actual cycling loading ratio and therefore it was decided to use each beam both for cycling and static testing (of course after symmetry and unbiased loading of the rig was evident from the first tests). This was carried out by heavily stiffening one of the test sections, so that it would be damaged as little as possible during the cycling loading phase up to the total collapse of the other test section. Then, this section was utilized for the ultimate static test in the inverted manner described earlier. 3 pairs of strain gage rosettes were bonded face to face on both sides of the shear web. They were located at the two "critical" zones at each end of the tension diagonal as close as possible to the frame, and at the center of the panel(Fig. 2). This latter one was used for reference measurements, as well as for determining the buckling load and overall average behavior of the beam.

4. NUMERICAL STUDIES

The STAGS computer program [21] was chosen for numerical support of the research.

Calculations of the buckling load and postbuckling behavior of the panels and surrounding structure were conducted for beams WB-3 through WB-8 and WB-11. The analytical model used to represent the tested field of beams WB-3, WB-4 and WB-7 was a 160×160×0.5 mm plate attached to a stiffening frame comprising of a thicker plate with a width of 20 mm and thickness of 4.5 mm. (The need to replace the L stiffeners by a thicker plate stems from the inability of the STAGS version used in the calculation to account for the in-plane rigidity of the stiffeners).

For beams WB-5 and WB-11, the dimensions of the plate were 160×160×0.8 mm and the thickness of the frame was 4.8 mm, and for beams WB-6 and WB-8, the dimensions of the plate were 160×160×1.0 mm and the thickness of the frame was 5.0 mm.

The plate was attached to elastic beams which simulated the properties of the vertical stiffeners (uprights) and flanges of the tested beams (see Fig. 3 and Table 3).

The vertical stiffeners were loaded uniformly by distributed shear. In addition, forces normal to the cross section of the flanges, were introduced to simulate the bending moment acting on the beam.

The plate was discretized into a 29×29 non uniform grid with denser meshes at the corners.

The numerical analysis with the STAGS was performed in the two follo-
wing modes:

a. A bifurcation analysis to predict the buckling load of the shear webs
    of the beam. The initial buckling load is essential to the analysis
    of the repeatedly buckled beams.

b. An elastic nonlinear postbuckling analysis with assumed initial im-
    perfections to support and supplement the test results. An important ob-
    jective of this phase of the numerical analysis was also the definition
    of the shear load V_y where yielding first occurs at the critical lo-
    cations near the tension diagonal.

The buckling load yielded by the numerical studies with STAGS was com-
pared with the calculated buckling load obtained with Eq 32 of Ref. 3 and
with the actual buckling load observed at the test. These critical loads
are given in Table 2.

In the early studies with STAGS, the imperfection w_0 of the web was
taken as a one term half sine wave in the x and y directions.

$$w_0(x,y) = a_0 \sin\left(\frac{\pi x}{d}\right) \sin\left(\frac{\pi y}{b}\right)$$

The choice of imperfection mode was for the purpose of observing the deve-
lopment and emergence of changing buckling and post-buckling deformation
patterns. Application of this imperfection mode has indicated that severe
convergence problems were encountered unless an imperfection amplitude a_0
of a magnitude equal to the thickness of the web was introduced into the
calculations. Also, increasing experience with the above one term imper-
fection, $w_0(x,y)$, proved it to be insufficient for studying the post buckling

behavior of the beam. Therefore, the following two term expression

$$w_0(x,y) = a_0 (\sin \frac{\pi x}{d} \sin \frac{\pi y}{b} + 0.25 \sin \frac{2\pi x}{d} \sin \frac{2\pi y}{b})$$

was adopted for further studies with the STAGS program.

In the numerical studies, the shear load V was increased in increments up to a maximum shear which was well over the working cyclic loading. The maximum load for WB-3, WB-4 and WB-7 was 1400 kg and for WB-5 and WB-11, the load was 1500 kg. No convergence problems were encountered in this range.

The computed load-vs-deflections curves as well as the corresponding experimental curves are shown in Fig. 4 and Fig. 5 for WB-3 and WB-5 respectively. The somewhat higher deformations obtained in the numerical calculations are probably due to the more severe imperfection used in the calculations (compared with the experiments) and slightly more flexible support conditions. Apart from this, the numerical results follow the test results quite well.

In Figs. 6 and 7 the calculated deflected shapes along the two diagonals of the web of beam WB-3 at different load levels, are compared with the test results. A good correlation between the predicted shapes and the experimental results, is observed. The scatter at some points is due to difficulties in analysing the moiré records in particular in the small deflection range. Similar results were obtained for the other tested beams.

The deflected pattern of beam WB-7 obtained from the STAGS program for V = 600 kg is presented in Fig. 8 and compared with the corresponding

test results. The highly stressed "critical" regions, where the cracks initiate, are indicated in the figure.

5. TEST RESULTS - DISCUSSION & ANALYSIS.

The test results are presented in Table 2, together with the pre-
dicted results using the numerical studies with STAGS [21] and those
calculated according to Ref. [3].

a. Buckling loads.

The experimental buckling loads $(V_{cr})_{exp}$, were obtained from load-
strain responses, recorded by a pair of strain gages bonded face to face
at the center of the web (see Section 3). The critical loads were deter-
mined by the method described in Fig. 9 for beam WB-11. It is seen from
this table that a rather good agreement exists between the calculated loads
by the two methods of analysis and that correlation between the theoreti-
cal predictions and the experimental buckling load depend upon the relative
rigidity of the frames.

Fair agreement is observed for the beams with the "heaviest" frames,
WB-3, WB-4 and WB-7, whereas very good correlation is found for the beams
with the relatively moderate stiffening, WB-5, WB-6, WB-8 and WB-11, and
the most flexible frames WB-9 and WB-2. This implies that the actual
rigidity of the stiffeners in the experiments is less than that assumed
in the calculations. The effect is more pronounced in the case of the
heavier stiffeners, which (theoretically) should have approached the
case of fixed supports.

A typical moiré fringe picture of a buckled web showing the deflection
pattern at the buckling load is given in Fig. 10 for beam WB-6. The shape

of the buckling mode is in agreement with the results of the STAGS cal-
culations. It can be useful for further improved calculations.

b. Ultimate failure load.

In the static ultimate tests it was observed that collapse of the beams
was associated with two different modes of failure: Shearing of the web
along a diagonal perpendicular to the tension field in beams WB-3, WB-4,
WB-5 (see Fig. 11), or failure of the flanges of the beam, either in
yielding or buckling for the rest of the beams (see Fig. 12). It is seen
from Table 2, that neither of these modes of failure had a definite effect
on the agreement between the predicted ultimate loads (eq.2 of Ref.[3]) and
the experimental ones. However, the correlation for the beams which failed
in the "tearing mode", resulted in a ratio of the experimental load to
the calculated load which was equal to, or greater than unity, whereas
the ratios for the other beams varied between values smaller than unity
and above unity.

It should be noted that the flanges of beams WB-6 and WB-8 experienced
local bucklings at loads which were considerably below the predicted ul-
timate loads (see Table 2). After this behavior was observed for beam
WB-6 (and later for beam WB-8), loading of beam WB-8 was stopped immedia-
tely at incipient buckling. The beam was unloaded, its compression flange
was stiffened and the beam was subsequently reloaded untill collapse.
It is apparent from Table 2 that stiffening of the flange had a signifi-
cant effect on the failure load of the beam and resulted in a load almost
equal to the predicted one.

c. Repeated bucklings.

Table 2 presents the number of cycles N_i to initiation of a crack at the critical corner (as actually first observed during the test; see later discussion), and the number of cycles N_f to complete failure of the shear web for the prescribed cyclic loading conditions represented by (V_{ult}) cal.$/V_{cyclic}$ and V_{cyclic}/V_{cr}.

During the repeated buckling tests, cracks were first detected, as expected, at the lower corner of the web along the tension diagonal, except for beam WB-11 where the crack was first observed at the upper corner of the diagonal. These cracks whre, when observed, of a length of about ten times the thickness of the web and it is reasonable to assume that they were formed by the severe bending stresses on the tension bending side at the corner.

Since these cracks formed at the very edge of the web almost under the stiffeners and they first developed by propagation through the thickness of the web from the tension to the compression side, their detection was almost impossible before they have reached a certain length and depth. Therefore, the value of N_i should be regarded with caution. Also it was observed that at this stage, the cracks mainly propagated through the thickness of the web and were almost "steady" lengthwise. After comprehensive penetration through the thickness, the cracks began growing lengthwise and their growth was measured (see Fig. 13). The cracks started either horizontally and immediately followed by a vertical branch or vice versa.

As can be seen from Table 2 the rate of growth of the crack and the marginal cyclic life of the beam to reach N_f depended upon the working load ratio, V_{cyclic}/V_{ult}, yielding low N_f-N_i values for relatively high load ratios. It was also observed that in the case of low load ratios the cracks propagated lengthwise in a non continuous fashion up to complete failure, whereas for the higher ratios, the behavior was quite smooth.

d. Correlation studies.

The aim of the present work is to obtain design charts for predictions of durability of post buckled shear webs and design recommendations. Therefore, an attempt was made to establish a design curve from the present test results and the corresponding analytical studies. It has been tentatively assumed that the durability of the shear web is mainly governed by the following nondimensional parameters: V_{cyclic}/V_{cr} ; V_{ult}/V_{cyclic} ; $b^3 t/I_f$; according to the relation:

$$N_f = A \left(\frac{V_{cyclic}}{V_{cr}}\right)^\alpha \left(\frac{V_{ult}}{V_{cyclic}}\right)^\beta \left(\frac{b^3 t}{I_F}\right)^\gamma$$

It should be noted that based on the discussion regarding the accuracy in N_i in the previous paragraph, it seems to be more meaningful to predict N_f rather than N_i.

A least-square method was used to obtain the values of A, α, β, γ, which resulted in: A = 0.81, α = -0.81, β = 4.91, γ = 0.86.

It is seen from Table 2 that N_f for beam WB-3 deviates significantly

from the value that might be expected based on the N_f values experienced

for the identical beams WB-4 and WB-7. Note that beams WB-4 and WB-7

yielded N_f = 22300 at a working load of 900 kg and N_f = 168410 at a

working load of 600 kg respectively. The corresponding values for WB-3

were N_f = 23000 at 700 kg. This last result for N_f appears to be un-

reasonable, since a much higher value was expected. The possibility of

a defective beam should be considered and a retest is scheduled. This

deviation also affected significantly the least square results, when it

was included in the studies. Therefore it was excluded from the analysis.

6. CONCLUSIONS AND RECOMMENDATIONS FOR FUTURE WORK.

1. At load levels within the flight envelope (27% to 46% of ultimate loads), repeated buckling led to initiation (N_i) and propagation of fatigue cracks, with subsequent failure (N_f). Typical values of numbers of load cycles N_i and N_f ranged from about 20,000 cycles to 200,000 cycles. These values demonstrate the seriousness of the problem to the current design of flight vehicles.

2. Cracks started at the most highly stressed regions (as verified by the numerical analysis and by observed curvatures of the wave patterns) at the corners near the tension diagonals, along the attachment lines to the stiffeners and flanges.

3. A design formula was developed, which can predict $\log N_f$ in this test series to within a scatter of 19%.

4. From the formula, it appears that the most significant parameter affecting N_f was the ratio of V_{ult}/V_{cyclic}. The effects of the other parameters were close to linear.

5. An increase in the relative rigidity of the frames <u>reduced</u> the life N_f of the structure. Thus, it seems that over-rigidity of the supporting frames near the corners may lead to premature failure.

6. Good agreement was obtained between the test results and the supporting numerical analysis. This can be seen from comparisons of the deflection patterns of the web, (in Figs. 6, 7, and 8).

7. Based on the current results and conclusions, investigations are being persued in the following directions:

    a. Design formulas are now being developed for predicting crack initiation (N_i), based on an experimental "standardized" minimum crack size.

    b. A similar investigation will be conducted on the critical crack size and on the rate of crack propagation.

    c. An investigation will be conducted on the influence of additional parameters and their predictive capability. An important possibility in this respect which is now under study is V_y, which is the shearing load at which local yielding first starts at the location of crack initiation.

    d. Efforts to improve the numerical and analytical support capabilities are now being made.

- 25 -

ACKNOWLEDGEMENTS

REFERENCES

1. Ari-Gur, J., Singer, J. and Libai, A., "Repeated Buckling Tests of Stiffened Thin Shear Panels", Technion, Israel Inst. of Technology, Dept. of Aeronautical Engineering, TAE Report No. 463, August 1981.

2. Wagner, H., "Ebene Blechwandträger mit sehr dünnem Stegblech", Zeitschrift für Flugtechnik und Motorluftsch., Vol. 20, Nos. 8,9,10,11,12, 1929, translation: "Flat Sheet Metal Girders with very Thin Metal Web", NACA TM Nos. 604-606, 1931.

3. Kuhn, P., Peterson, J.P. and Levin, L.R. "A Summary of Diagonal Tension, Part I - Methods of Analysis, NACA TN 2661, May 1952.

4. Kuhn, P. Peterson, J.P. and Levin, L.R., "A Summary of Diagonal Tension, Part II - Experimental Evidence, " NACA TN 2662, May 1952.

5. Kuhn, P., Stresses in Aircraft and Shell Structures, McGraw-Hill, New York, 1956.

6. Hertel, H., Leichtbau, Springer, Berlin/New York, 1960.

7. Rockey, K.C., "Plate Girder Design - Flange Stiffness and Web Plate Behavior", Engineering, December 1957, pp. 788-792.

8. Mason, P.W., Balders, T. and Armen, H. Jr., "The Application of Non-linear Analysis Techniques to Practical Structural Design Problems", Computers and Structures, Vol. 16, No. 1-4, pp. 549-562, 1983.

9. Mueller, J.A. and Yen, B.T., "Girder Web Boundary Stresses and Fatigue", Welding Research Council Bulletin, No. 127, January 1968.

10. Patterson, P.J., Corrado, J.A., Huang, J.S. and Yen, B.T., "Fatigue and Static Tests of Two Welded Plate Girders", Welding Research Council Bulletin No. 155, October 1970.

11. Parsanejed, S. and Ostapenko, A., "On the Fatigue Strength of Unsymmetrical Steel Plate Girders", Welding Research Council Bulletin, No. 156, pp. 48-59, November 1970.

12. Saff, C.R., "Ultimate Strength and Permanent Buckling Analysis of Integrally Stiffened Shear Webs", McDonnell Aircraft Company Report, No. MDC A2587, December 1973, Also: Memorandum 237-611, 1975.

13. Agarwal, B.L., "Postbuckling Behavior of Composite Shear Webs", AIAA Journal, Vol. 19, No. 7, pp. 933-939, 1981.

14. Renieri, M.P. and Garrett, R.A., "Postbuckling Behavior of Flat Stiffened Graphite/Epoxy Shear Panels", MCAIR Rep. No. 81-015, McDonnell Aircraft Company, St. Louis, Missouri, January 1981.

15. Vestergren, P., "A Theoretical and Experimental Investigation of the Buckling Behavior of Rectangular CFRP Panels Subjected to Shear Loading, Report FFA HU-1818, The Aeronautical Research Inst. of Sweden, Stockholm, 1977.

16. Vestergren, P., "Skjuvprov med U-Balkar av Kolfiberarmerad Plast" (Shear Load Tests on U-Beams Made of Carbon Fiber Reinforced Plastic), Report FFA HU-1941, The Aeronautical Research Inst. of Sweden, Stockholm 1977.

17. Ivanson, S., Jarfall, L., Samuelson, A. and Gamziukas, V., "Nonlinear Analysis of Rectangular Panel Subjected to Shear Loads", The Aeronautical Research Inst. of Sweden, Report FFA HU-1893, August 1976.

18. Denke, P.H., "Strain Energy Analysis of Incomplete Tension Field Web-Stiffener Combinations", Journal of the Aeronautical Sciences, Vol. 11, No. 1, pp. 25-40, January 1944.

19. Kudva, N.J. and Agarwal, B.L., "Postbuckling Analysis of Stiffened Composite Shear Panels - Theoretical Analysis and Comparisons with Experiments", Proceedings of the Winter Annual Meeting of the ASME Structures and Materials, 1981.

20. McCormick, C.W. (ed), "The NASTRAN User's Manual, NASA SP-222(01), Washington, D.C., 1973.

21. Almroth, B.D., Brogan, F.A., Meller, E., Zale, F. and Petersen, H.T., "Collapse Analysis for Shells of General Shape: User's Manual for the STAGS-A Computer Code", AFFDL TR-71-8, March 1973.

22. Stein, M. and Starnes, J.H., "Numerical Analysis of Stiffened Shear Webs in the Postbuckling Range", Numerical Solution of Nonlinear Structural Problems, Hartung, R.F. (ed.), ASME, pp. 211-223, November 1973.

23. Vestergren, P. and Knutsson, L., "Theoretical and Experimental Investigations of the Buckling and Postbuckling Characteristics of Flat Carbon Fibre Reinforced Plastic (CFRP) Panels Subjected to Compression or Shear Loads," ICAS 1978, Proceedings of the 11th Congress of the International Council of the Aeronautical Sciences, Singer, J. and Staufenbiel, R. (eds.), Lisboa, Portugal, pp. 217-223, September 1978.

24. Samuelson, L.A., Vestergren, P., Knutsson, L., Wangberg, K.G. and Gamziukas, V., "Stability and Ultimate Strength of Carbon Fiber Reinforced Plastic Panels", Proceeding of International Congress on Composite Materials (ICCM/3), Paris, pp. 327-341, August 1980.

Table 1 : Dimensions of Test Specimens

Specimen	Frame size (mm)	web thickness t (mm)	b/t	I_f/b^3f	J_f/bt^3
WB-2	L×12×12×1	0.5	400	3.5×10^{-4}	4.0
WB-3	L×12×12×2	0.5	400	2.15×10^{-3}	22.4
WB-4	L×20×20×2	0.5	400	2.15×10^{-3}	22.4
WB-5	L×20×20×2	0.?	250	1.41×10^{-3}	6.3
WB-6	L×20×20×2	1.0	200	1.16×10^{-3}	3.6
WB-7	L×20×20×2	0.5	400	2.15×10^{-3}	22.4
WB-8	L×20×20×2	1.0	200	1.16×10^{-3}	3.6
WB-9	L×15×15×1.5	0.5	400	7.81×10^{-4}	7.7
WB-10	L×15×15×1.5	0.5	400	7.81×10^{-4}	7.7
WB-11	L×20×20×2	0.8	250	1.41×10^{-3}	6.3

Table No. 2 Predictions and Test Results

Beam	$(V_{cr})_{exp}$	$V_{cr}[3]$**	$V_{cr}[2i]$**	$(V_{ult})_{exp}$	$V_{ult}[3]$**	V_{cyc}	$\dfrac{V_{cyc}[3]}{V_{cr}[3]}$	$\dfrac{V_{ult}[3]}{V_{cyc}}$	N_i	N_f
WB-3*	75	98.4	105.8	2375	2208	700	7.11	3.15	18690	23000
WB-4	80	98.4	105.8	2500	2208	900	9.15	2.45	14000	22308
WB-7	75	98.4	105.8	8**	2208	600	6.10	3.68	88000***/120000	1684108**/212700
WB-5	370	388.6	388.8	3290	3324	1250	3.22	2.66	100000	119235
WB-11	374	388.6	388.6		3324	1350	3.47	2.46	63100	66000
WB-6	660	715.4	729.4	3800	4143	1900	2.66	2.18	25000	32457
WB-8	640	715.4	729.4	3300****, 4062	4143	1700	2.38	2.44	91200	108690
WB-9	83.6	89.6	-	-	1600	600	6.70	8.67	35000	83750
WB-10	-	89.6	-	1800	1600	720	8.04	2.22	24220	29410
WB-2	75	75	-	1290	1330	700	9.33	1.90	88583	10271

* For geometry of the beams see Table 1

** Calculated according to corresponding reference

*** No ultimate failure test, cyclic test carried out for both panels of the beam

**** Ultimate load before stiffening of flange

Table 3   Properties of beams WB-3, WB-5, WB-6 for STAGS analysis.

		WB-3	WB-5	WB-6
t_1	web thickness	0.5 mm	0.8 mm	1.0 mm
t_2	flange and upright thickness	4.5 mm	4.8 mm	5.0 mm
A_F	flange cross-section area	162 mm^2	168 mm^2	172 mm^2
A_U	upright cross-section area	162 mm^2	168 mm^2	172 mm^2
I_{ZF}	flange moment of inertia about z axis	6264 mm^4	6557 mm^4	6786 mm^4
I_{yF}	flange moment of inertia about y axis	11208 mm^4	11485 mm^4	11674 mm^4
I_{ZU}	upright moment of inertia about z axis	6264 mm^4	6557 mm^4	6786 mm^4
I_{yU}	upright moment of inertia about axis	11208 mm^4	11485 mm^4	11674 mm^4
J_{xF}	flange torsional moment of inertia, x axis	326.4 mm^4	324 mm^4	328 mm^4
J_{yU}	upright torsional moment of inertia, y axis	326.4 mm^4	324 mm^4	328 mm^4
GJ_{yF}	torsional stiffness	9.3×10 kgmm^2	9.4×10 kgmm^2	9.5×10 kgmm^2
GJ_{xU}	torsional stiffness	9.3×10 kgmm^2	9.4×10 kgmm^2	9.5×10 kgmm^2
e	position of the force arm (Fig. 3)	6.0 mm	6.1 mm	5.8 mm
$\dfrac{B'}{d'}$		0.26596	0.26624	0.26624

Note: The inplane portions of the L stiffeners are included in their
properties.
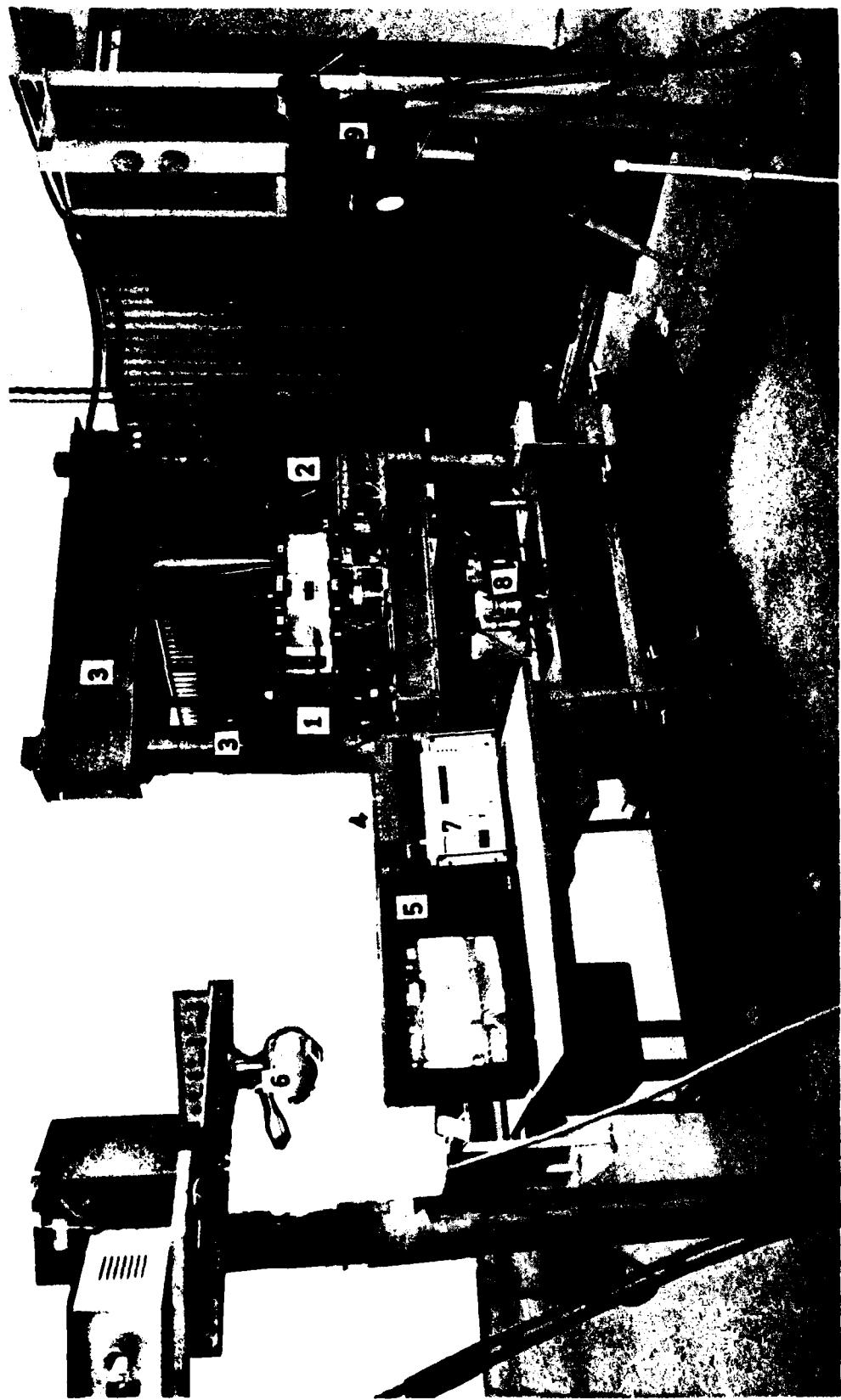
1 - tested specimen
2 - cross members for lateral displacements prevention
3 - loading frame
4 - video recorder
5 - T.V. monitor

6 - Moire lamp
7 - multichannel data logger
8 - MTS hydraulic jack
9 - camera

Fig. 1 TEST SET-UP
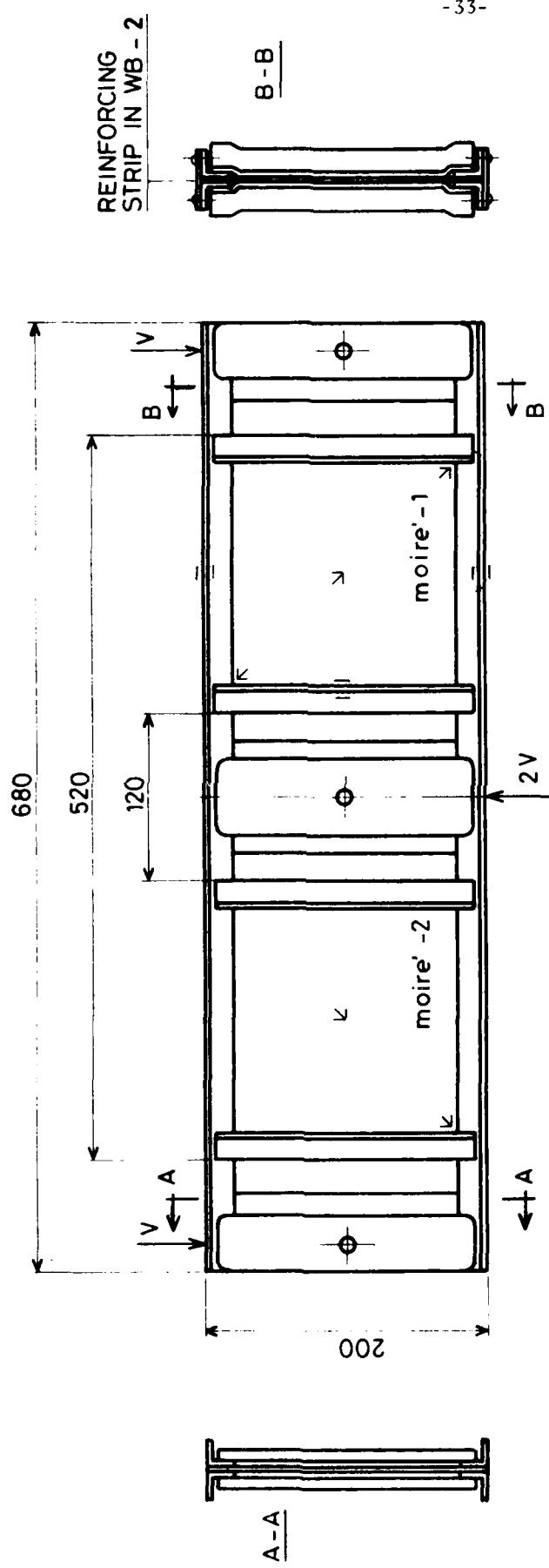
Fig. 2 WAGNER BEAMS OF TEST SERIES
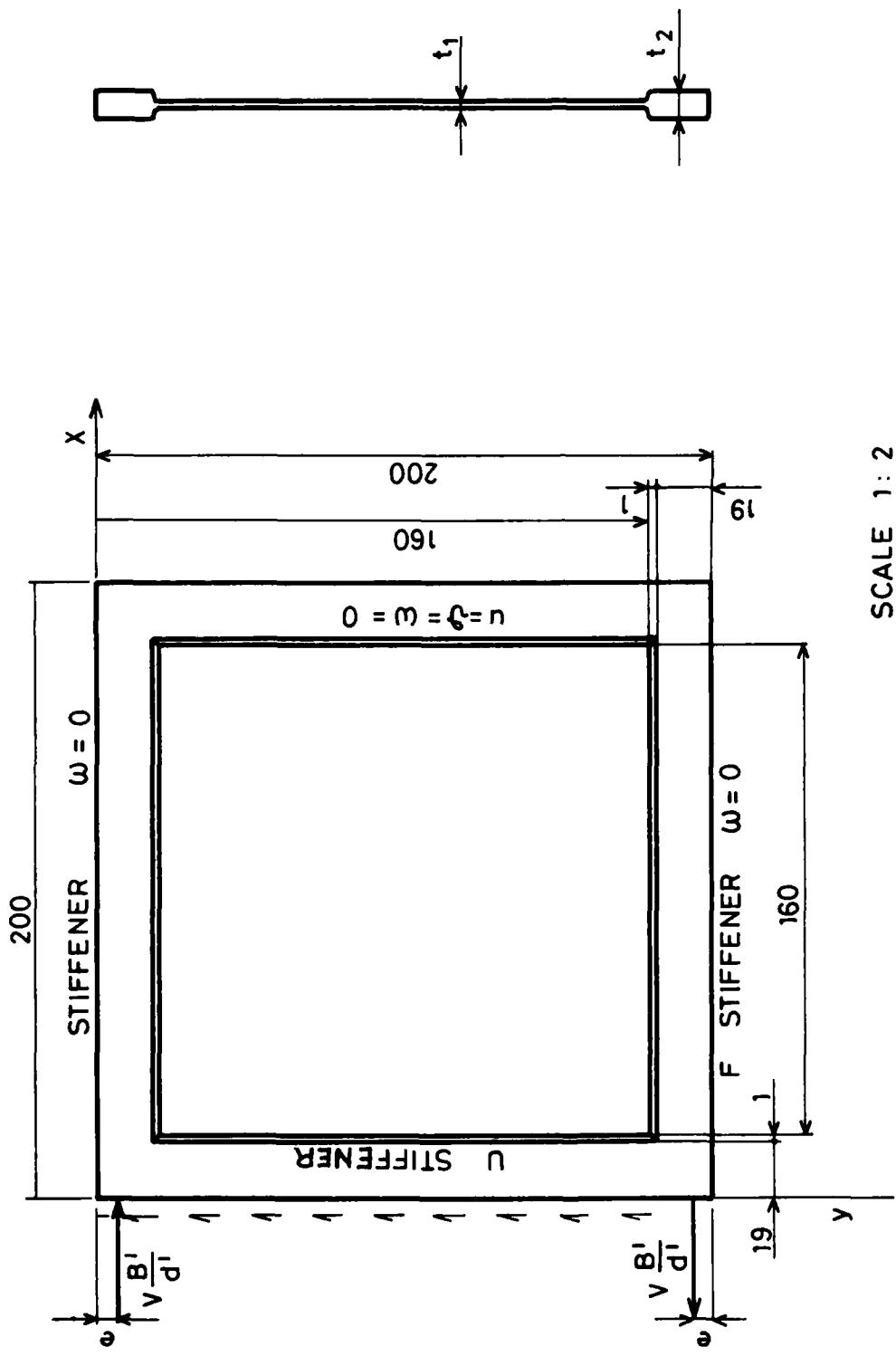
Fig. 3 MODEL FOR NUMERICAL STUDY BY STAGS PROGRAM

See Table 3, p. 31.
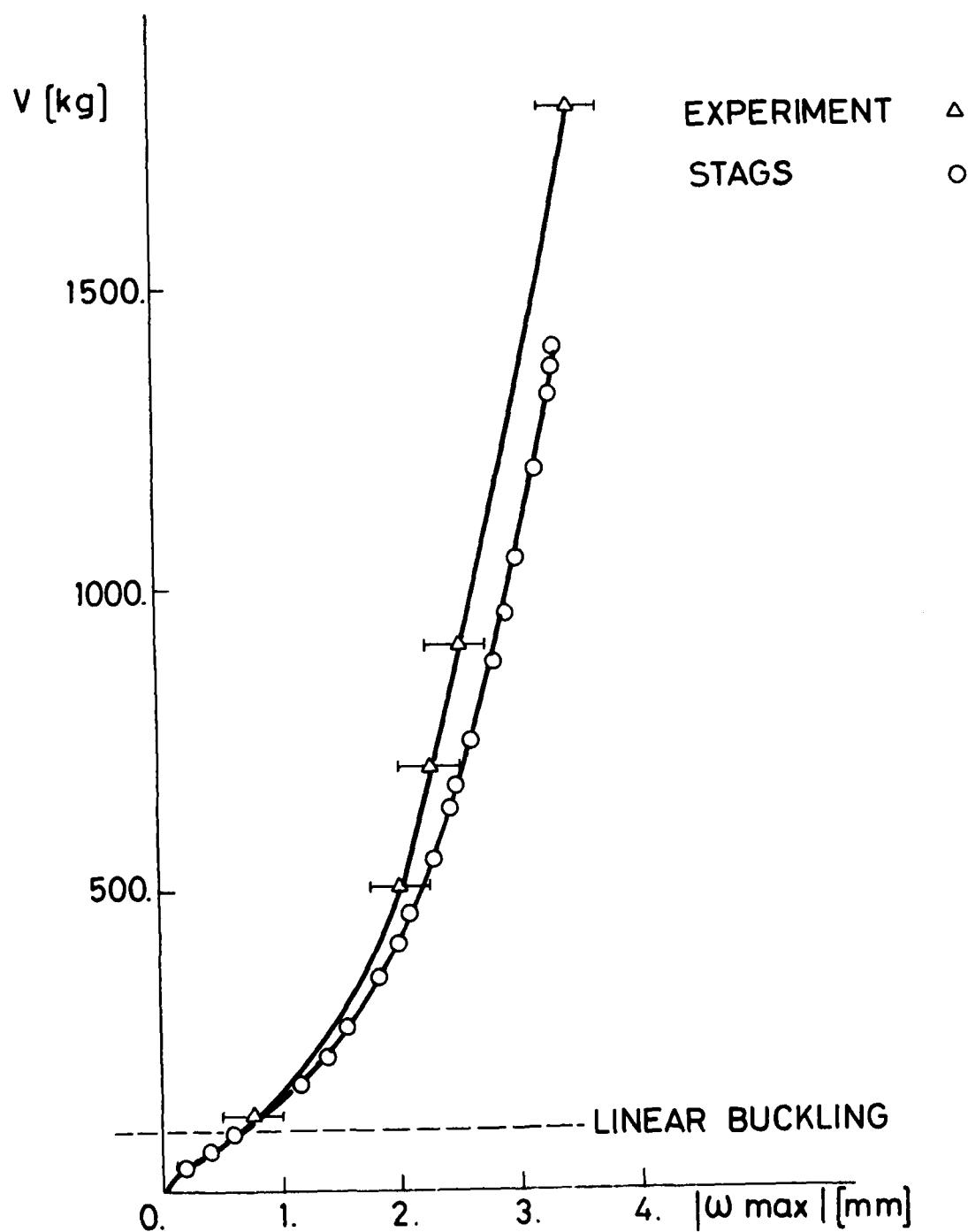
Fig. 4   EXPERIMENTAL AND COMPUTED LOAD-DEFLECTION CURVES OF WB-3.
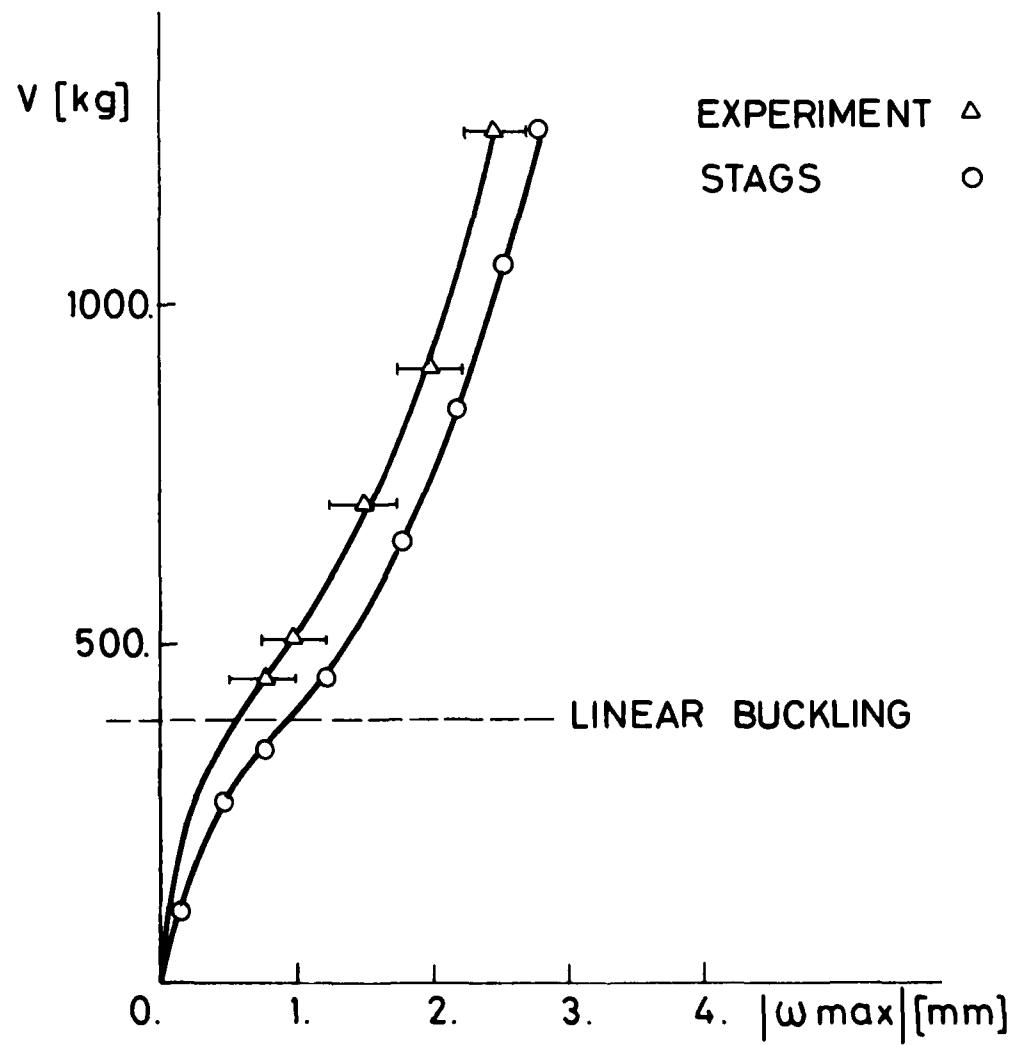
Fig. 5 EXPERIMENTAL AND COMPUTED LOAD DEFLECTION CURVES OF WB-5.
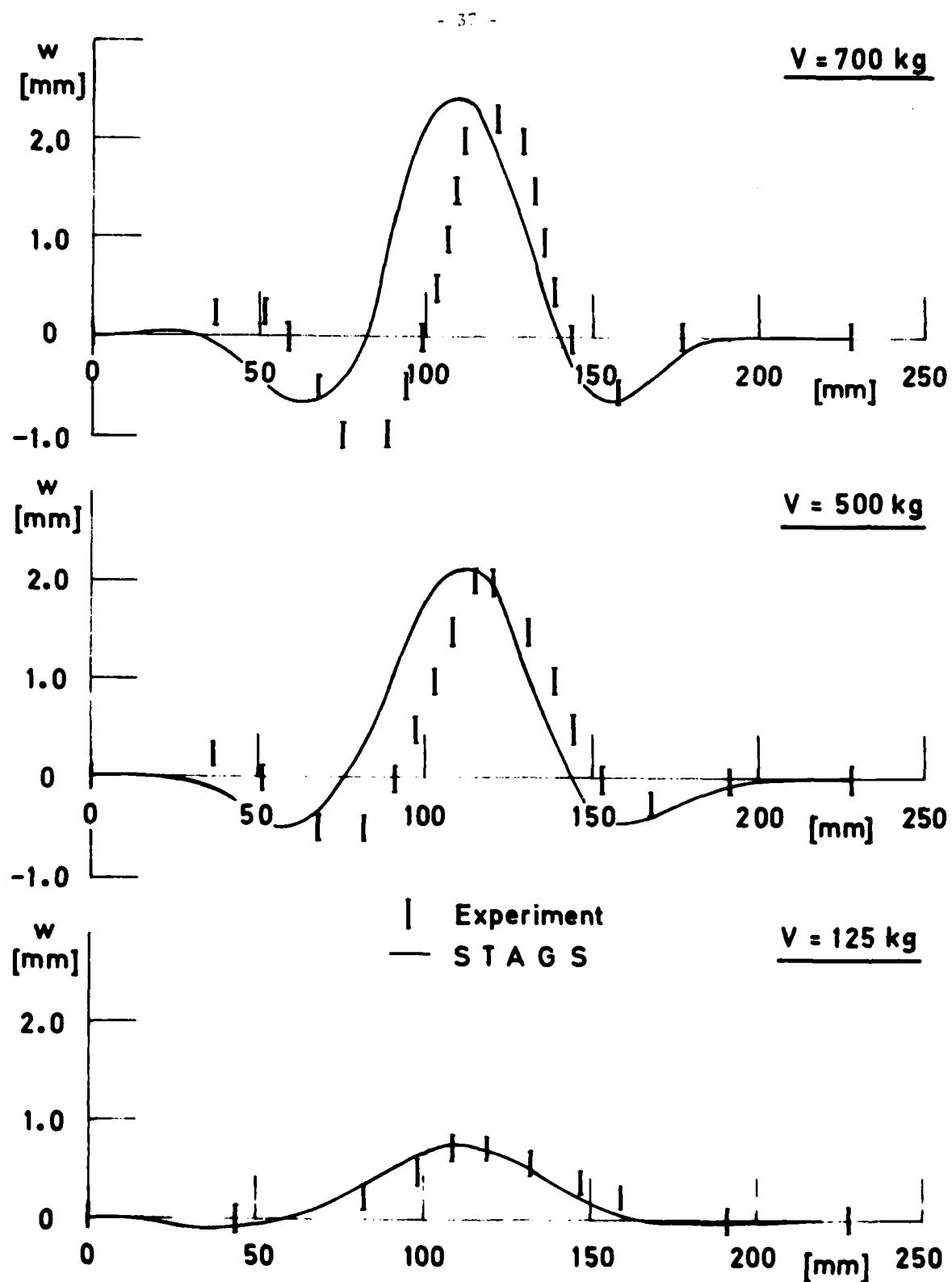
Fig. 6 EXPERIMENTAL AND COMPUTED LATERAL DEFLECTIONS ALONG THE COMPRESSION DIAGONAL (BEAM WB-3).
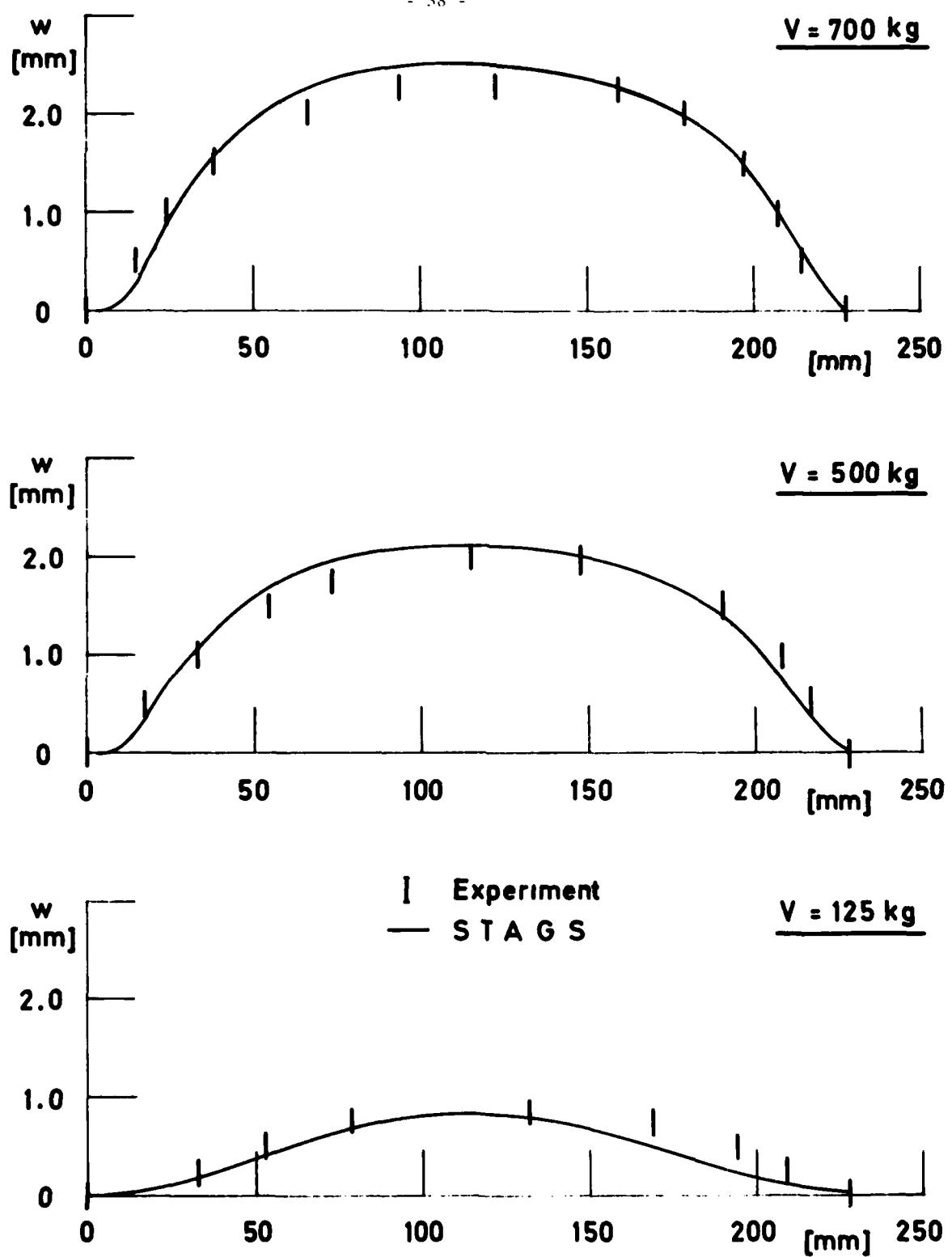
Fig. 7 EXPERIMENTAL AND COMPUTED LATERAL DEFLECTIONS ALONG THE TENSION DIAGONAL (BEAM WB-3).
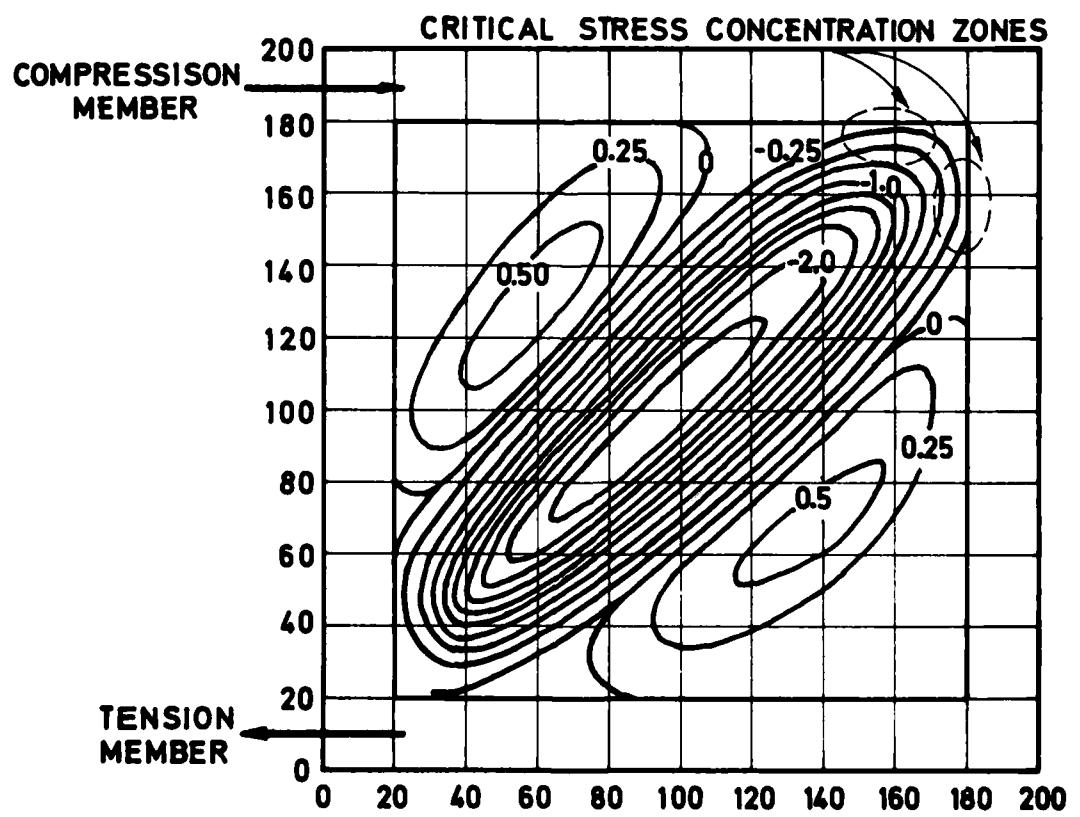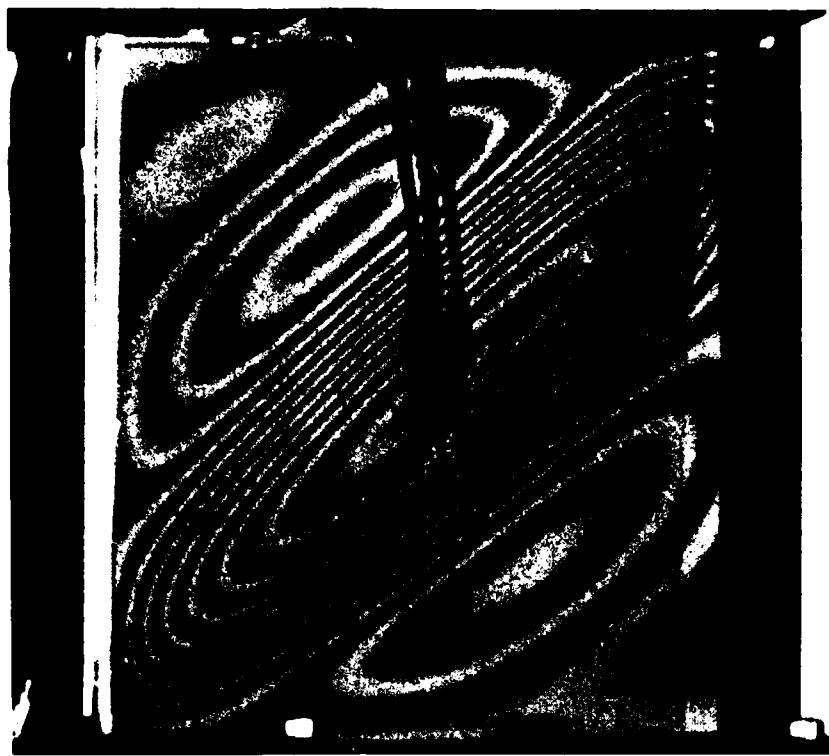
Fig. 8 EXPERIMENTAL AND COMPUTED DEFLECTION PATTERN (BEAM WB-7).
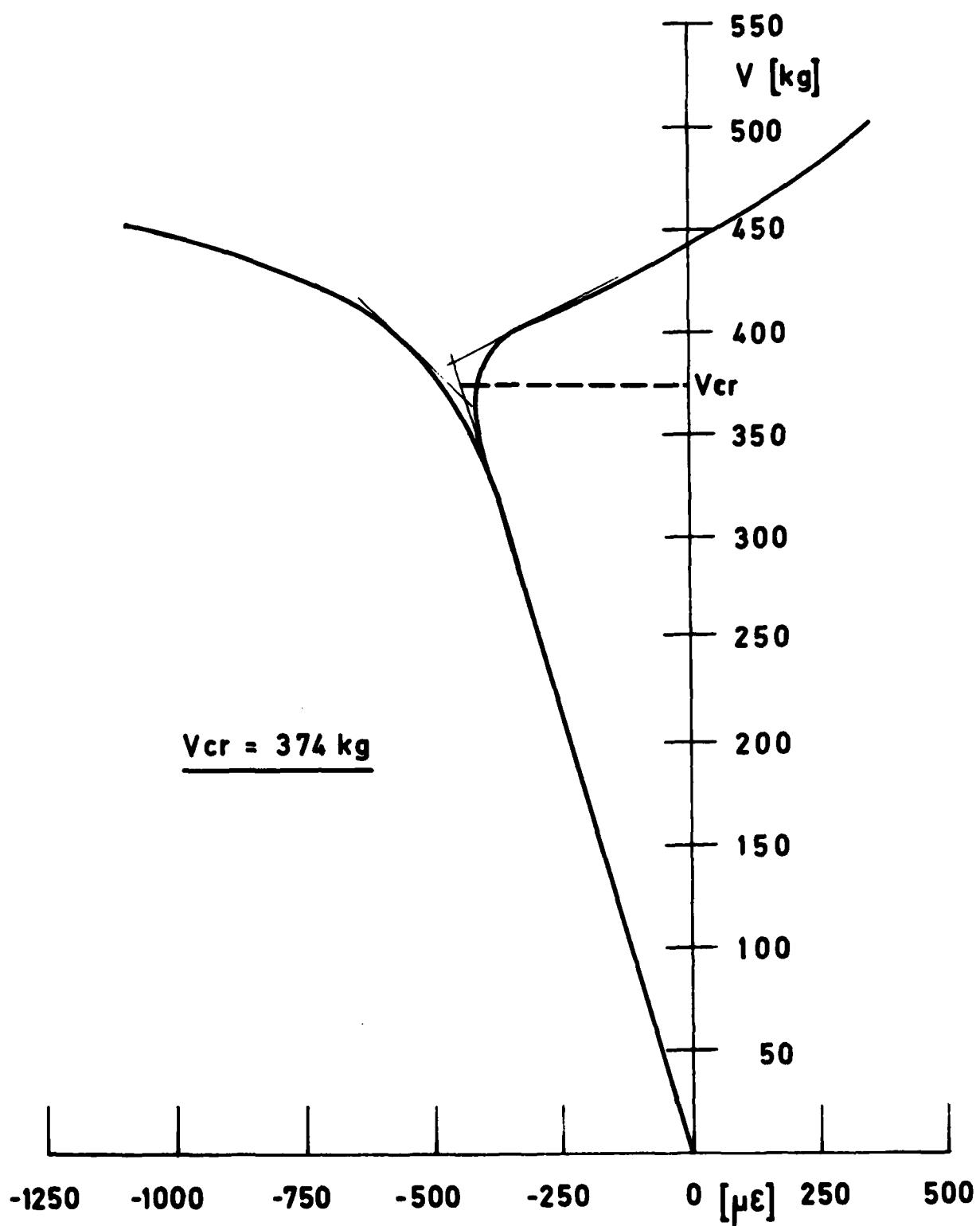
Fig. 9   EXPERIMENTAL DETERMINATION OF CRITICAL LOAD   (BEAM WB-11).
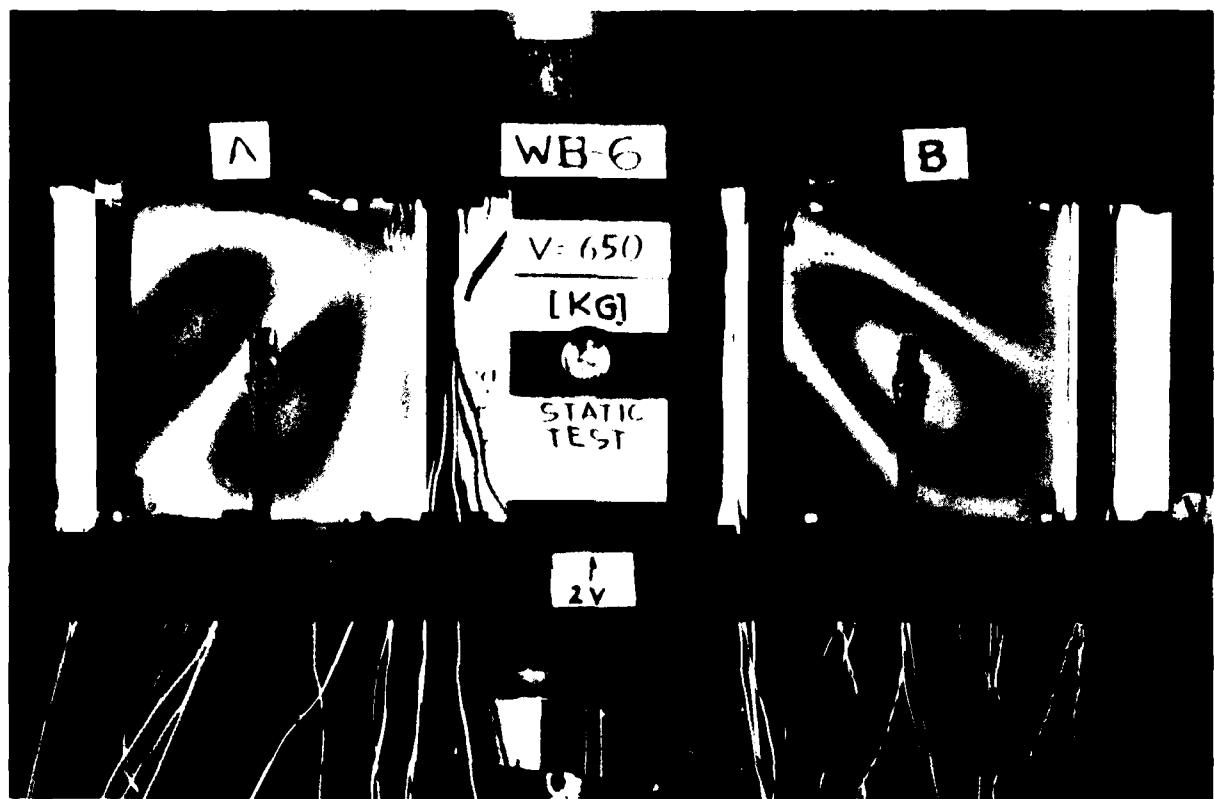
Fig. 10   MOIRE FRINGE PICTURE OF BUCKLED WEB AT CRITICAL LOAD (BEAM WB-6).

Fig. 11 TYPICAL "TEARING FAILURE" MODE
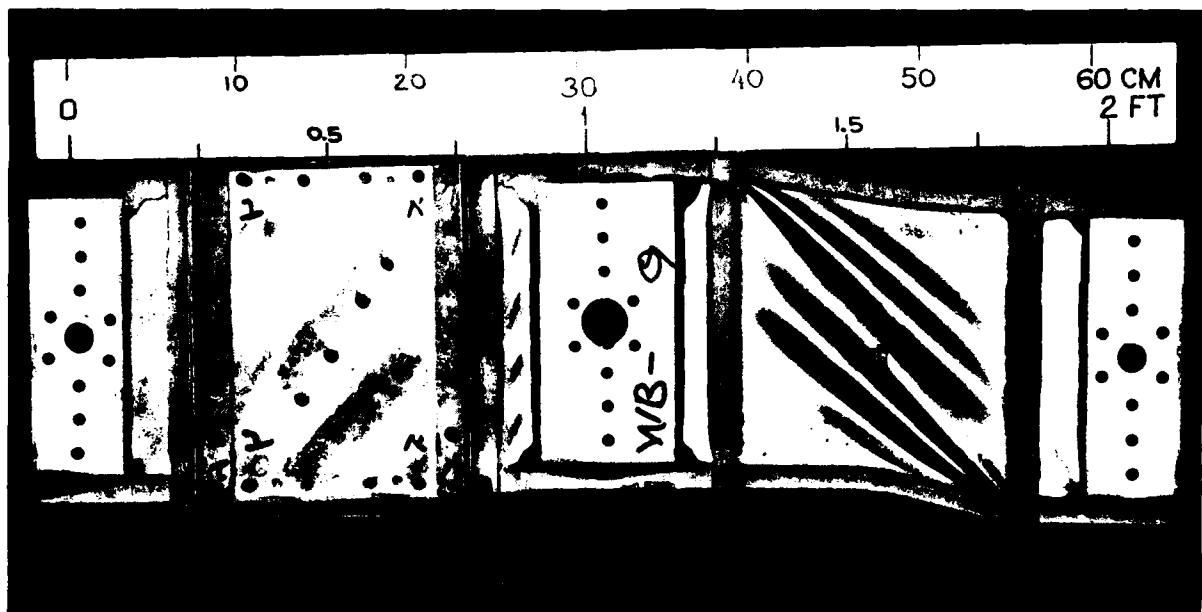
Fig. 12 TYPICAL FAILURE MODE IN BENDING AND BUCKLING OF THE FLANGE
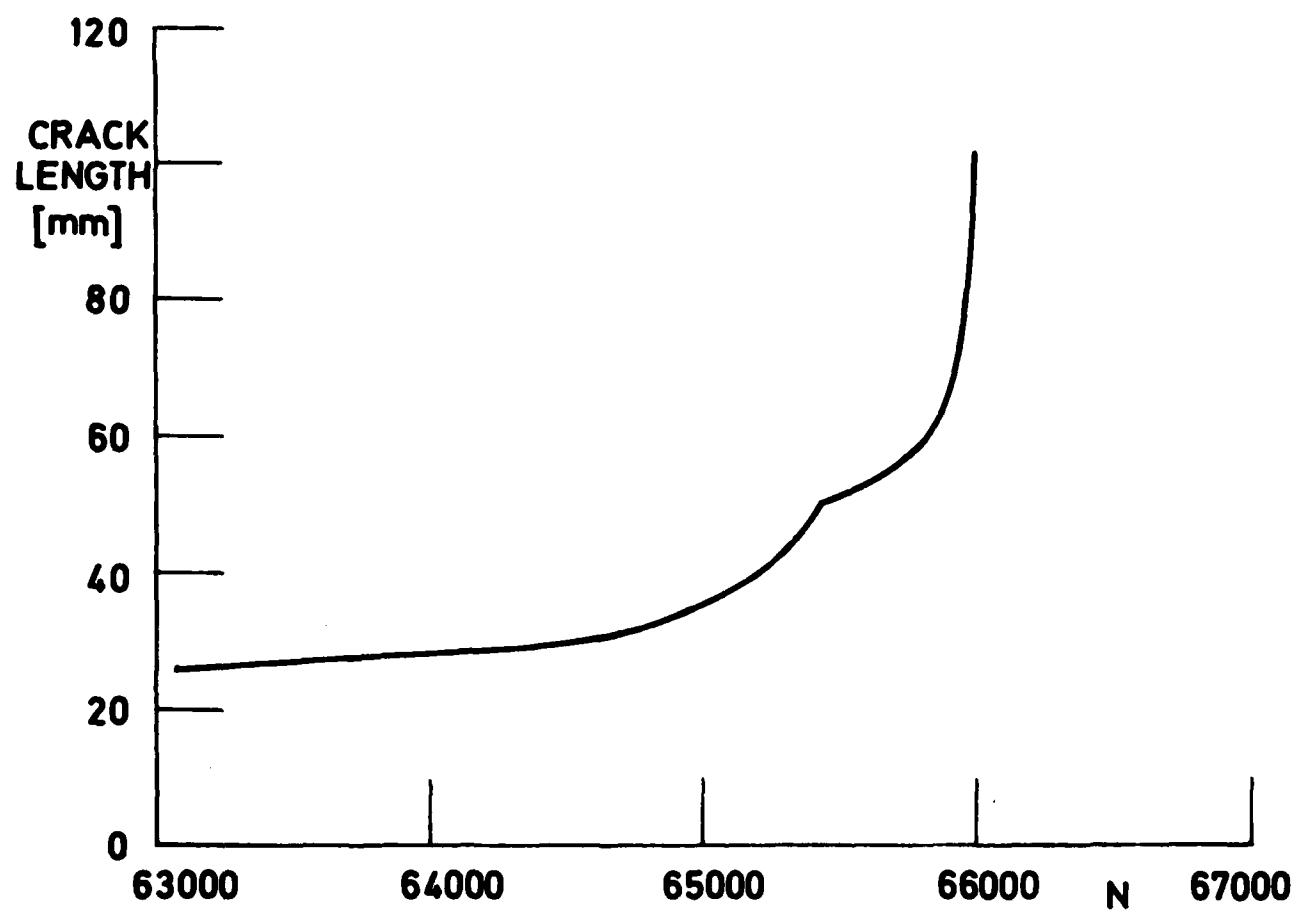
Fig. 13   CRACK LENGTH VERSUS NUMBER OF CYCLES

END

DTIC

6 - 86